Derivatization of inhibitor of apoptosis protein (IAP) ligands yields improved inducers of estrogen receptor α degradation

Received for publication, November 22, 2017, and in revised form, February 6, 2018 Published, Papers in Press, March 15, 2018, DOI 10.1074/jbc.RA117.001091

Nobumichi Ohoka[‡], Yoko Morita[§1], Katsunori Nagai[§1], Kenichiro Shimokawa[§], Osamu Ujikawa[§1], Ikuo Fujimori[§], Masahiro Ito[§], Youji Hayase[§], Keiichiro Okuhira[‡2], Norihito Shibata[‡], Takayuki Hattori[‡], Tomoya Sameshima[§], Osamu Sano[§], Ryokichi Koyama[§3], Yasuhiro Imaeda[§], Hiroshi Nara[§4], Nobuo Cho[§5], and Mikihiko Naito[‡6]

From the [‡]Division of Molecular Target and Gene Therapy Products, National Institute of Health Sciences, Kanagawa 210-9501 and the [§]Pharmaceutical Research Division, Takeda Pharmaceutical Co. Ltd., Kanagawa 251-8555, Japan

Edited by George N. DeMartino

Aberrant expression of proteins often underlies many diseases, including cancer. A recently developed approach in drug development is small molecule-mediated, selective degradation of dysregulated proteins. We have devised a protein-knockdown system that utilizes chimeric molecules termed specific and nongenetic IAP-dependent protein erasers (SNIPERs) to induce ubiquitylation and proteasomal degradation of various target proteins. SNIPER(ER)-87 consists of an inhibitor of apoptosis protein (IAP) ligand LCL161 derivative that is conjugated to the estrogen receptor α (ERα) ligand 4-hydroxytamoxifen by a PEG linker, and we have previously reported that this SNIPER efficiently degrades the ERα protein. Here, we report that derivatization of the IAP ligand module yields SNIPER(ER)s with superior protein-knockdown activity. These improved SNIPER(ER)s exhibited higher binding affinities to IAPs and induced more potent degradation of ERα than does SNIPER(ER)-87. Further, they induced simultaneous degradation of cellular inhibitor of apoptosis protein 1 (cIAP1) and delayed degradation of X-linked IAP (XIAP). Notably, these reengineered SNIPER(ER)s efficiently induced apoptosis in MCF-7 human breast cancer cells that require IAPs for continued cellular survival. We found that one of these molecules, SNIPER(ER)-110, inhibits the growth of MCF-7 tumor xenografts in mice more potently than the previously characterized SNIPER(ER)-87. Mechanistic analysis revealed that our novel SNIPER(ER)s preferentially recruit XIAP, rather than cIAP1, to degrade ERα. Our results suggest that derivatized IAP ligands could facilitate further development of SNIPERs with potent protein-knockdown and cytocidal activities against cancer cells requiring IAPs for survival.

Aberrant or increased expression of pathogenic proteins often results in the initiation of many diseases, including a variety of cancers. However, a limited number of pathogenic proteins are currently targeted by pharmacological inhibitors, primarily because many proteins do not have suitable binding pockets where a pharmacophore may interact to regulate protein activity (1, 2). An alternative approach has been to down-regulate expression of the pathogenic proteins; this is usually achieved *in vitro* through use of genetic methods involving antisense oligonucleotides, dsRNAs, and CRISPR-Cas9 technology. However, clinical application of these technologies remains challenging because delivery of oligonucleotides to the target tissues is not easily accomplished (3, 4).

As a novel strategy to down-regulate pathogenic proteins in a nongenetic manner, we and others have devised a protein-knockdown system that uses small molecules with sufficient membrane permeability to induce selective degradation of target proteins. These small-molecule compounds, designated as proteolysis-targeting chimeras (PROTACs)[7] and specific and non-genetic IAP-dependent protein erasers (SNIPERs), are chimeric molecules that contain two different ligands connected by a linker; one ligand is specific for an E3 ubiquitin ligase, and the other is specific for a target protein (5–7). The PROTACs and SNIPERs are designed to cross-link the E3 ubiquitin ligase and the target protein to induce polyubiquitylation and proteasomal degradation of the target protein within cells. To recruit the von Hippel–Lindau (VHL) E3 ligase complex and the cereblon (CRBN) E3 ligase complex, a VHL inhibitor (based on the HIF-1α peptide) and a phthalimide moiety have been

This work was supported in part by grants from the Japan Society for the Promotion of Science (KAKENHI Grants 26860049 (to N. O.) and 16H05090 and 16K15121 (to M. N.)), the Japan Agency for Medical Research and Development (AMED Grants JP 17ak0101073 (to M. N.) and JP17cm0106124 and JP17ak0101073 (to N. O.)), and Takeda Science Foundation (to N. O.). Y. M., K. N., K. S., O. U., I. F., M. I., Y. H., T. S., O. S., R. K., Y. I., H. N., and N. C. are employees of Takeda Pharmaceutical Co. Ltd.
This article contains Tables S1 and S2 and Figs. S1–S7.

[1] Present address: Axcelead Drug Discovery Partners, Inc., Kanagawa 251-0012, Japan.
[2] Present address: Institute of Biomedical Sciences, Tokushima University Graduate School, Tokushima 770-8505, Japan.
[3] Present address: SCOHIA PHARMA, Inc., Kanagawa 251-8555, Japan.
[4] Present address: The Pharmaceutical Society of Japan, Tokyo 150-0002, Japan.
[5] Present address: Drug Discovery Chemistry Platform Unit (Wako branch), RIKEN Center for Life Science Technologies, Saitama 351-0198, Japan.
[6] To whom correspondence should be addressed: Division of Molecular Target and Gene Therapy Products, National Institute of Health Sciences, 3-25-26 Tonomachi, Kawasaki, Kanagawa 210–9501, Japan. Tel: 81-44-270-6533; Fax: 81-44-270-6534; E-mail: miki-naito@nihs.go.jp.

[7] The abbreviations used are: PROTAC, proteolysis targeting chimera; BIR, baculoviral IAP repeat; BRD4, bromodomain-containing protein 4; cIAP1, cellular inhibitor of apoptosis protein 1; CRBN, cereblon; DIABLO, direct IAP-binding protein with low pI; FBS, fetal bovine serum; mAb, monoclonal antibody; pAb, polyclonal antibody; PI, propidium iodide; SMAC, second mitochondria-derived activator of caspases; SNIPER, specific and non-genetic IAP-dependent protein eraser; VHL, von Hippel–Lindau; XIAP, X-linked inhibitor of apoptosis protein; ERα, estrogen receptor α; PARP, poly(ADP-ribose) polymerase; TNF, tumor necrosis factor.

respectively integrated into PROTAC constructs (8–11). In a similar manner, an IAP antagonist has been incorporated into SNIPERs to recruit either cellular inhibitor of apoptosis protein 1 (cIAP1) or X-linked inhibitor of apoptosis protein (XIAP) E3 ligase (12–18). To date, a range of PROTAC and SNIPER compounds have been developed, allowing degradation of a variety of proteins, such as estrogen receptor α (ERα), oncogenic kinase BCR-ABL, and epigenetic regulator bromodomain-containing protein 4 (BRD4) (19–30). Some PROTACs and SNIPERs also have demonstrated the ability to degrade target proteins *in vivo*, suggesting that this technology is feasible for use in novel drug development. These include VHL-based and CRBN-based PROTACs directed against BRD4, which are capable of inducing BRD4 protein degradation in mouse xenograft models (10, 31). By incorporating an LCL161 derivative, a high-affinity IAP ligand, we developed SNIPER(ER)-87, which induces *in vivo* degradation of ERα and growth inhibition of an ERα-positive human breast tumor in a xenograft model (13).

IAPs are a family of antiapoptotic proteins containing one or three baculoviral IAP repeat (BIR) domains (32–34). Some family members, such as cIAP1, cIAP2, and XIAP, directly interact with and regulate caspases via the BIR domain, thus inhibiting apoptosis (35–38). These IAPs are attractive targets for tumor therapy because of their frequent overexpression in multiple human malignancies and their implications in tumor progression, treatment failure, and poor prognosis (39–45). Based on the IAP-binding tetrapeptides of second mitochondria-derived activator of caspases/direct IAP-binding protein with low pI (SMAC/DIABLO), many potent and cell-permeable peptidomimetic IAP antagonists (also known as SMAC mimetics) have been developed; some of these are under evaluation in clinical phase studies as antitumor drugs (32, 46, 47). These IAP antagonists interact with BIR domains in IAP proteins to directly inhibit XIAP or to induce autoubiquitylation and proteasomal degradation of cIAP1 and cIAP2 (48–51). Because SNIPERs utilize IAP antagonists as IAP-ligand modules, SNIPERs are able to down-regulate IAPs beyond the initial target proteins (12–18); this is likely to be advantageous when attempting to kill cancer cells that require IAPs for survival.

In this paper, we demonstrate that, by derivatizing the IAP-ligand module, we have developed novel SNIPER(ER)s whose protein knockdown and antitumor activities are more potent than those of SNIPER(ER)-87. These SNIPER(ER)s have higher affinity for IAPs and exhibit more consistent abilities to degrade ERα and IAPs. In addition, we discuss the significance of IAP down-regulation in pharmacological efforts to induce cancer cells to undergo apoptosis.

Results

Structure-activity relationship of SNIPER(ER)s with novel IAP ligands

To discover IAP ligands that are useful for the development of SNIPERs with potent protein-knockdown activity, we substituted the IAP ligand moiety of SNIPER(ER)-87 with several IAP antagonists that have been reported elsewhere (52–55) (Fig. 1 and Table S1) and examined their abilities to reduce ERα expression by MCF-7 human breast tumor cells (Fig. 2). In a series of SNIPER(ER)s with different IAP ligand modules, we found that five compounds (SNIPER(ER)-105 (**4**), -110 (**31a**), -113 (**31c**), -119 (**31d**), and -126 (**50**)) reduced ERα expression comparably with, and more potently than, SNIPER(ER)-87 for durations of 4 and 48 h, respectively (Fig. 2*a*). SNIPER(ER)-130 (**69**) and -131 (**71**) exhibited attenuated knockdown activities, whereas the others (SNIPER(ER)-104 (**9**), -118 (**55a**), -121 (**55b**), -134 (**31b**), and -136 (**40**)) did not induce effective knockdown at 1–100 nM (Fig. 1*b*). The DC_{50} (the concentration required for 50% reduction of expression) for each SNIPER(ER) compound is summarized in Table 1.

Table 1 also reports the binding affinities (IC_{50}) of SNIPER(ER)s to ERα and IAPs *in vitro*. Because SNIPER(ER)-87 preferentially recruits XIAP to degrade ERα (13), we compared the binding affinity to XIAP with the DC_{50}, for all SNIPER(ER)s. SNIPER(ER)s with effective knockdown activities (SNIPER(ER)-105, -110, -113, -119, and -126) exhibited affinities to XIAP that were greater than, or comparable with, that of SNIPER(ER)-87; in contrast, those with little or no ERα-knockdown activity (SNIPER(ER)-104, -118, -121, -134, and -136) exhibited lower binding affinities to XIAP. However, SNIPER(ER)-130 and -131 exhibited attenuated ERα-knockdown activities, despite their higher affinities for XIAP binding. These results suggest that an increased binding affinity of SNIPER(ER) for XIAP seems to be important for effective ERα knockdown but is not the sole determinant for degradation activity. Among the arene substitution isomers (SNIPER(ER)-110, -113, and -119), SNIPER(ER)-110 exhibited slightly better ability to degrade ERα; therefore, we chose SNIPER(ER)-110 as a representative. SNIPER(ER)-105, -110, and -126 also showed more potent ability to degrade ERα, compared with SNIPER(ER)-87, in assays involving other human ERα-positive breast tumor T47D and ZR-75-1 cells (Fig. 3).

Degradation of cIAP1 and XIAP by SNIPER(ER)s

As observed in studies of many IAP antagonists, SNIPERs in our study rapidly induced proteasomal degradation of cIAP1, along with degradation of their target proteins (12–18). SNIPER(ER)-105, -110, -113, -119, and -126 each reduced the cIAP1 level more potently than SNIPER(ER)-87 (Figs. 2*a* and 3*b*), consistent with their increased binding affinities for cIAP1 (Table 1). Further, these SNIPER(ER)s reduced XIAP expression in MCF-7 cells after 48 h in a more potent fashion than SNIPER(ER)-87 (Fig. 2*a*). The reduction of XIAP by SNIPER(ER)s was prominent in T47D cells after 48 h but was weak after 4 h of exposure (Fig. 3*b*). The difference in the degradation pattern between cIAP1 and XIAP suggests that these IAPs are degraded through a different mechanism, as discussed below.

XIAP is required for the ERα degradation by SNIPER(ER)s

We previously reported that XIAP is preferentially recruited to ERα upon treatment with SNIPER(ER)-87 (13). To examine which IAP is recruited by the novel SNIPER(ER)s (SNIPER(ER)-105, -110, and -126) to induce ERα degradation, MCF-7 and T47D cells were treated with or without the SNIPER(ER)s in the presence of MG132, a proteasome inhibi-

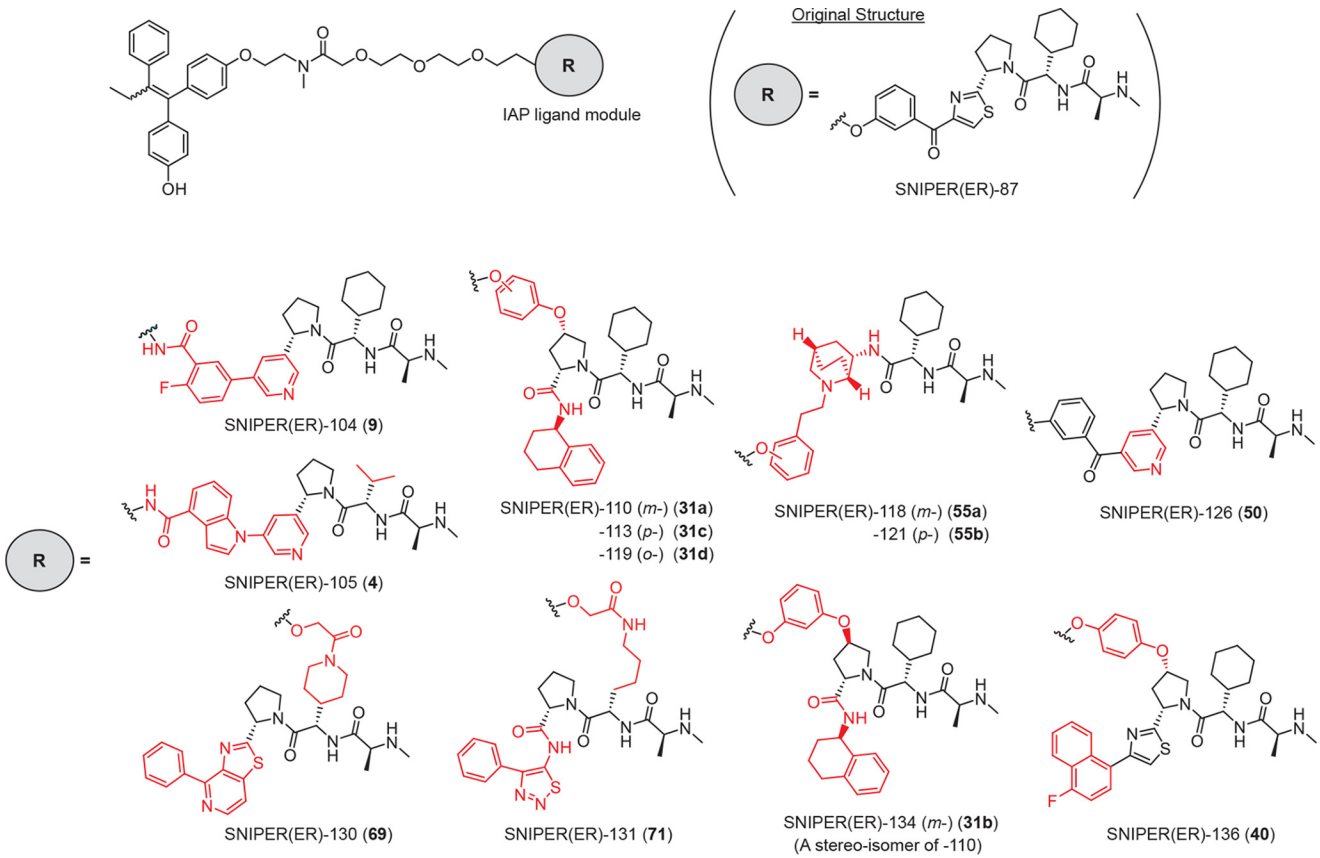

Figure 1. Chemical structures of novel SNIPER(ER)s. The IAP ligand moiety of SNIPER(ER)-87 was substituted by various IAP antagonists. Chemical structures shown in *red* indicate parts changed from the original SNIPER(ER)-87.

tor; cell lysates were analyzed by co-immunoprecipitation. Fig. 4*a* shows that, when cells were treated with SNIPER(ER)s, the anti-ERα precipitates contained both XIAP and cIAP1. We did not examine cIAP2, because it is not expressed in MCF-7 and T47D cells under normal cell culture and cIAP1-down-regulated conditions (Fig. S1, *a–c*). Upon comparison of IAP protein levels in total cellular lysates, we found that SNIPER(ER)s more effectively recruited XIAP to ERα, compared with cIAP1. Consistent with this, depletion of XIAP by siRNA substantially suppressed the ERα degradation induced in MCF-7 and T47D cells by our SNIPER(ER) molecules, whereas depletion of cIAP1 marginally suppressed the degradation (Fig. 4*b*). These results indicate that SNIPER(ER)-105, -110, and -126 preferentially recruit XIAP to degrade ERα in target cells, similar to the mechanism initiated by SNIPER(ER)-87.

SNIPER(ER)s induce apoptosis in tumor cells requiring IAPs for survival

Because ERα plays an important role in the proliferation of most primary breast tumors (56, 57), we examined the effect of SNIPER(ER)s on the growth of breast tumor cells. SNIPER(ER)s and fulvestrant, a clinically approved inducer of ERα degradation, both efficiently suppressed the growth of ERα-positive breast tumor cells (MCF-7 and T47D) but not of ERα-negative breast tumor cells (MDA-MB-231) (Fig. 5*a* and Fig. S2). Notably, SNIPER(ER)-105, -110, and -126 exhibited superior antiproliferative effects on MCF-7 cells at concentrations above 50 nM, compared with SNIPER(ER)-87 (Fig. 5*a* and Fig. S2). In a microscopic analysis, we observed that substantial number of MCF-7 cells, but not T47D cells, underwent cell death upon treatment with SNIPER(ER)-105, -110, and -126 (Fig. 5*b*). Induction of apoptotic cell death in MCF-7 cells by SNIPER(ER)-105, -110, and -126 was confirmed by flow cytometric analysis and annexin V/propidium iodide (PI) staining (Fig. 5 (*c* and *d*) and Fig. S3). Consistent with this, a 100 nM concentration of these SNIPER(ER)s activated caspase-7 and caspase-6 (detected by reduction of their precursor forms), which resulted in the cleavage of two caspase substrates, PARP and lamin B1, in MCF-7 cells (Fig. 5*e*). These results indicate that SNIPER(ER)-105, -110, and -126 each induced apoptosis in MCF-7 cells more effectively than SNIPER(ER)-87; apoptosis was not observed in T47D cells.

To understand why these new SNIPER(ER)s effectively induce apoptosis in MCF-7 cells, but not in T47D cells, and because SNIPER(ER)-105, -110, and -126 each induced the degradation of cIAP1 and XIAP more potently than SNIPER (ER)-87 (Figs. 2*a* and 3*b*), we investigated the effects of IAP depletion in MCF-7 and T47D cells. In MCF-7 cells, individual silencing of cIAP1 and XIAP by siRNA slightly reduced the number of cells; combined silencing of cIAP1 and XIAP reduced the number of cells by ~50%, compared with untreated cells (Fig. 6*a*), and was accompanied by caspase activation, as demonstrated by cleavage of lamin B1 and PARP (Fig. 6*b*). In contrast, similar silencing of IAPs in T47D cells neither reduced cell number nor activated caspases. When ERα was

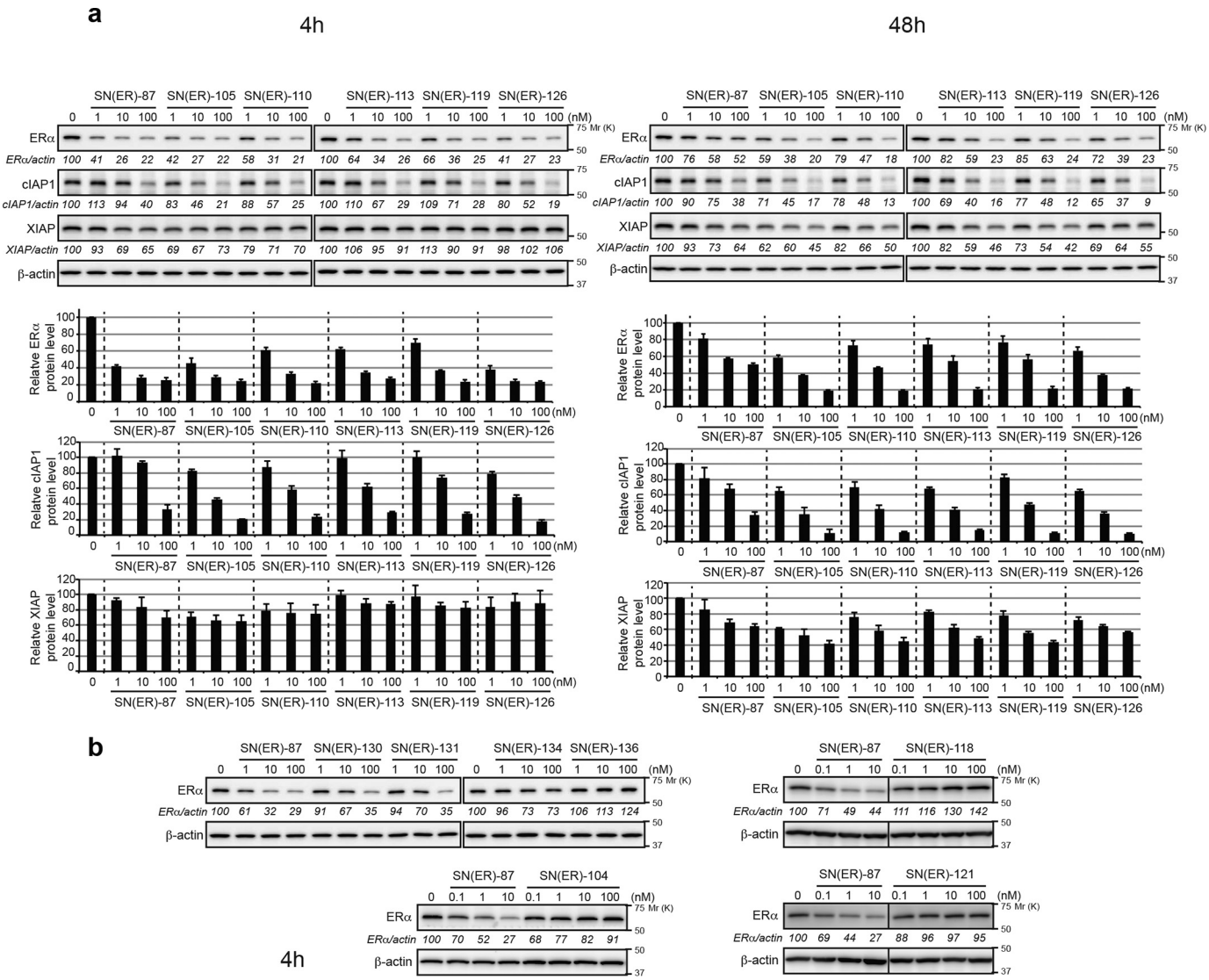

Figure 2. Novel SNIPER(ER)s with potent protein-knockdown activity. *a* and *b*, MCF-7 cells were treated with the indicated concentrations of SNIPER(ER)s for the indicated periods. Whole-cell lysates were analyzed by Western blotting with the indicated antibodies. *Numbers below* the *ERα*, *cIAP1*, or *XIAP panels* represent ERα/actin, cIAP1/actin, or XIAP/actin ratios, normalized by designating the expression from the vehicle control condition as 100%. *a*, data in the bar graph are the mean ± S.D. (*error bars*) of three independent experiments.

Table 1

Protein-knockdown activities and binding affinities of SNIPER(ER)s

Compound no.	ERα DC_{50}		IC_{50} (95% CI)				IAP ligand	
	4 h	48 h	ERα	cIAP1	cIAP2	XIAP	Originator	Reference
	nM		nM					
SNIPER(ER)-87	<3	83.0	110 (58–200)	450 (360–560)	960 (600–1500)	700 (510–960)	Novartis	WO2008016893
SNIPER(ER)-104	>100	ND[a]	61 (26–140)	>1000	>1000	>1000	Novartis	WO2012080260
SNIPER(ER)-105	<3	<3	69 (7–670)	5.3 (4.6–6.1)	7.2 (4.9–11)	55 (38–80)	Novartis	WO2012080271
SNIPER(ER)-110	<3	7.7	120 (68–200)	74 (62–89)	73 (55–97)	330 (250–430)	Abbott	Ref. 52; WO2016169989
SNIPER(ER)-113	<3	13.3	150 (82–290)	85 (75–96)	99 (58–200)	810 (58–200)	Abbott	Ref. 52; WO2016169989
SNIPER(ER)-118	>100	ND	230 (73–540)	140 (58–200)	900 (58–200)	>1000	AstraZeneca	Ref. 53
SNIPER(ER)-119	4	15.7	200 (73–540)	80 (62–100)	48 (28–82)	700 (490–1000)	Abbott	Ref. 52; WO2016169989
SNIPER(ER)-121	>100	ND	ND	650 (540–780)	>1000	>1000	AstraZeneca	Ref. 53
SNIPER(ER)-126	<3	3.7	83 (2–3800)	68 (66–77)	200 (150–280)	490 (310–760)	Novartis	WO2008016893
SNIPER(ER)-130	36.9	ND	41 (25–65)	68 (60–77)	28 (21–39)	25 (17–37)	Genentech	Ref. 54
SNIPER(ER)-131	33.8	ND	80 (39–160)	25 (22–28)	24 (18–32)	140 (85–220)	Genentech	Ref. 55
SNIPER(ER)-134	>100	ND	47 (15–140)	550 (450–670)	360 (240–540)	>1000	Abbott	Ref. 52
SNIPER(ER)-136	>100	ND	47 (25–89)	890 (790–1000)	>1000	>1000	Genentech	Ref. 54; WO2006069063

[a] ND, not determined.

silenced in MCF-7 and T47D cells, the numbers of cells in both cell lines were effectively reduced without a requirement for caspase activation. However, triple silencing of ERα, XIAP, and cIAP1 efficiently reduced MCF-7 cell number, compared with T47D cells; further, caspase activation was observed only in MCF-7 cells. Additionally, an IAP antagonist, LCL161, sensitized tumor necro-

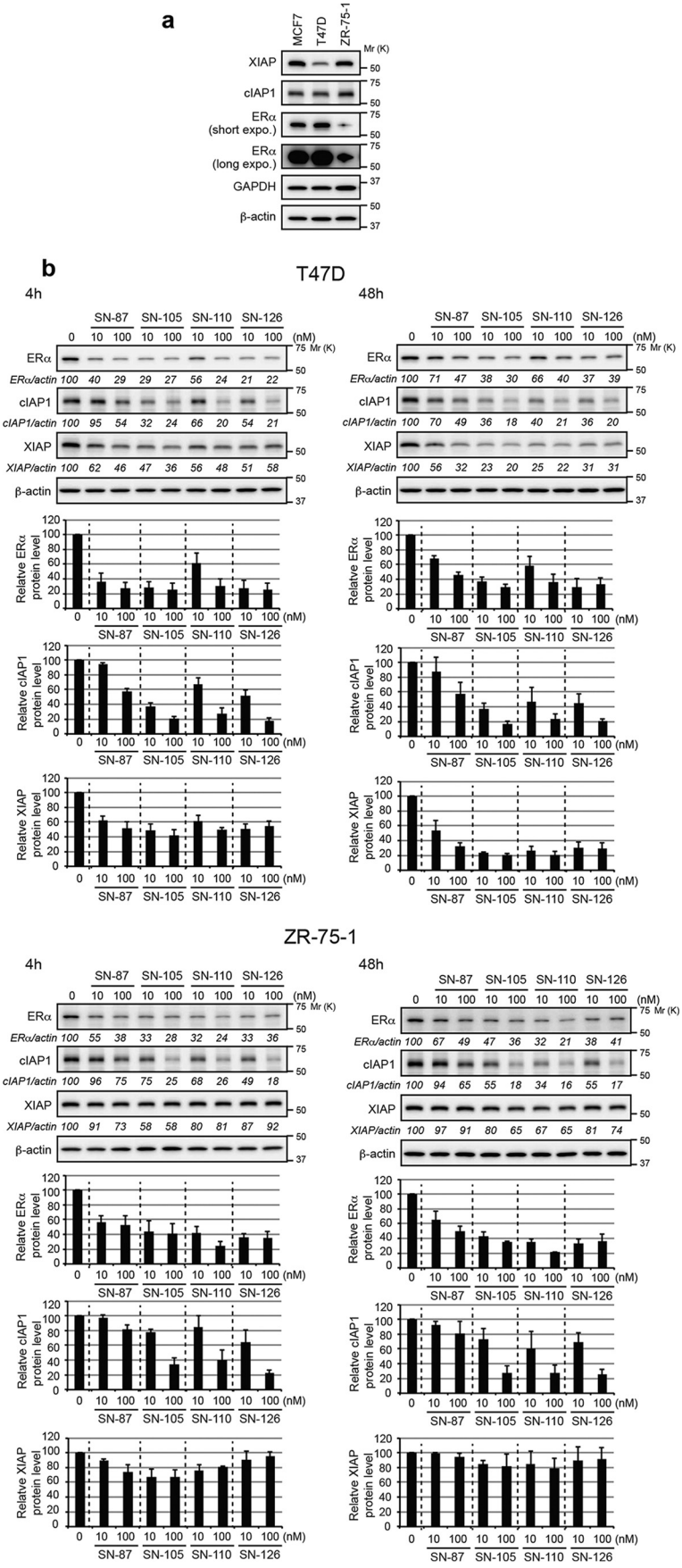
a
MCF7
T47D
ZR-75-1
Mr (K)
XIAP
cIAP1
ERα (short expo.)
ERα (long expo.)
GAPDH
β-actin
b
T47D
4h
48h
SN-87 SN-105 SN-110 SN-126
0 10 100 10 100 10 100 10 100 (nM)
ERα
ERα/actin 100 40 29 29 27 56 24 21 22
ERα/actin 100 71 47 38 30 66 40 37 39
cIAP1
cIAP1/actin 100 95 54 32 24 66 20 54 21
cIAP1/actin 100 70 49 36 18 40 21 36 20
XIAP
XIAP/actin 100 62 46 47 36 56 48 51 58
XIAP/actin 100 56 32 23 20 25 22 31 31
β-actin
Relative ERα protein level
Relative cIAP1 protein level
Relative XIAP protein level
ZR-75-1
4h
48h
ERα/actin 100 55 38 33 28 32 24 33 36
ERα/actin 100 67 49 47 36 32 21 38 41
cIAP1/actin 100 96 75 75 25 68 26 49 18
cIAP1/actin 100 94 65 55 18 34 16 55 17
XIAP/actin 100 91 73 58 58 80 81 87 92
XIAP/actin 100 97 91 80 65 67 65 81 74

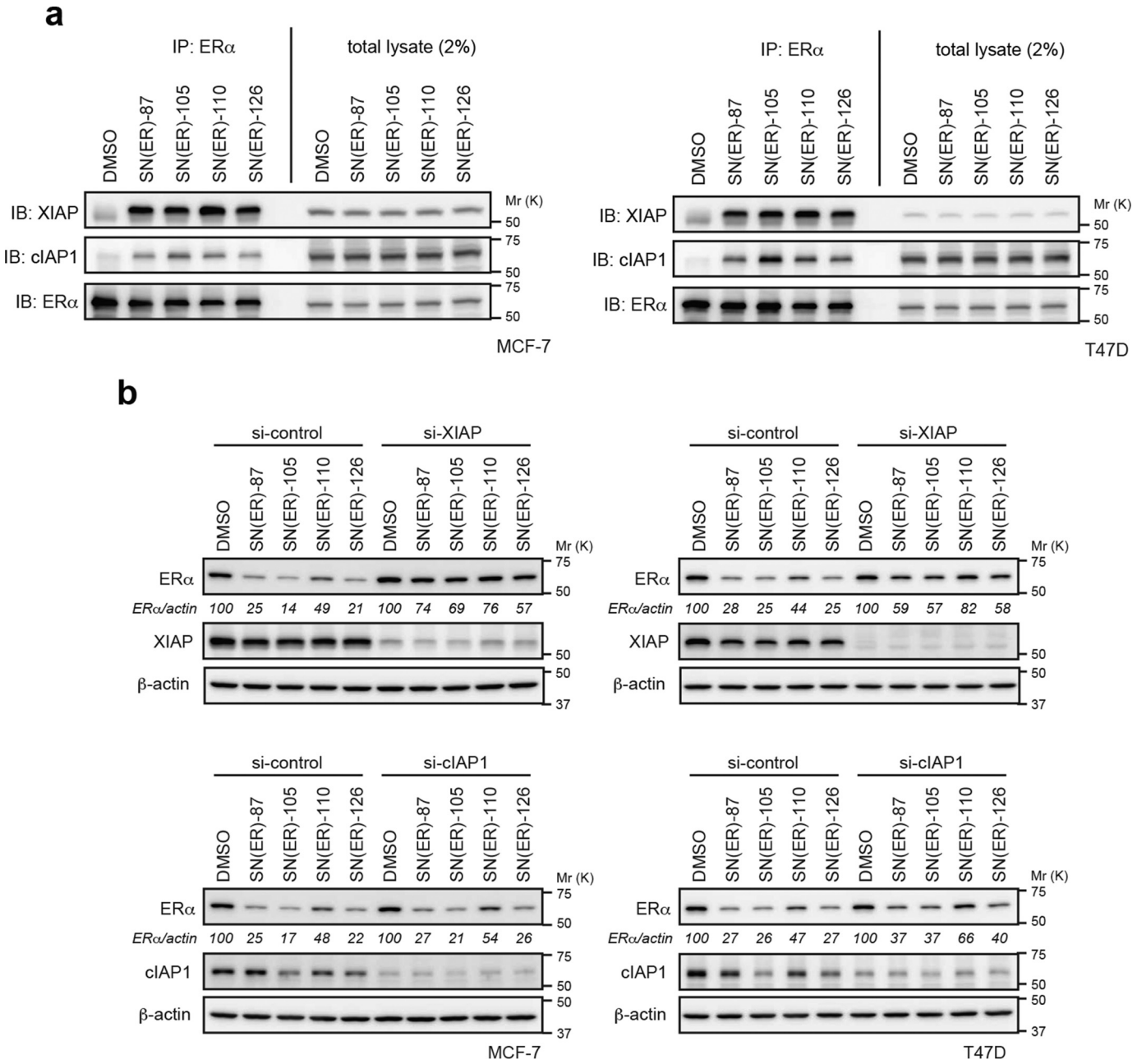

Figure 4. Role of XIAP in ERα degradation by SNIPER(ER)s. *a*, SNIPER(ER)s preferentially recruit XIAP to ERα. MCF-7 or T47D cells were treated with 10 nM SNIPER(ER)s in the presence of 10 μM MG132 for 3 h. Immunoprecipitates of anti-ERα (*IP*) and whole-cell lysates (*total lysates*) were analyzed by Western blotting (*IB*). *b*, depletion of XIAP suppresses the SNIPER(ER)-induced degradation of ERα. MCF-7 and T47D cells were transfected with the indicated siRNA for 42 h and treated with 10 nM SNIPER(ER)s for 3 h. Whole-cell lysates were analyzed by Western blotting with the indicated antibodies. *Numbers below* the *ERα panel* represent the ERα/actin ratio, normalized by designating the expression from the vehicle control condition as 100%. A mixture of three different siRNAs against each target was used to suppress expression.

sis factor α (TNFα)-dependent apoptosis in MCF-7 cells, but not T47D cells (Fig. S4). These results suggest that MCF-7 cells, but not T47D cells, require IAPs for survival; thus, IAPs could be involved in the selective induction of apoptosis in MCF-7 cells that have been exposed to SNIPER(ER)-105, -110, and -126.

In vivo protein-knockdown activities and antitumor activities of SNIPER(ER)s

We measured the metabolic stabilities of SNIPER(ER)-87, -105, -110, -113, -119, and -126 in liver microsomes (Table S2)

Figure 3. Protein-knockdown activities of SNIPER(ER)s in T47D and ZR-75-1 breast tumor cells. *a*, protein levels of IAPs and ERα in human ERα-positive breast tumor cells. *b*, knockdown activities of SNIPER(ER)s in T47D and ZR-75-1 cells. Cells were treated with the indicated concentrations of SNIPER(ER)s for the indicated periods. Whole-cell lysates were analyzed by Western blotting with the indicated antibodies. *Numbers below* the *ERα*, *cIAP1*, or *XIAP panels* represent ERα/actin, cIAP1/actin, or XIAP/actin ratios, normalized by designating the expression from the vehicle control condition as 100%. Data in the bar graph are the mean ± S.D. (*error bars*) of three independent experiments.

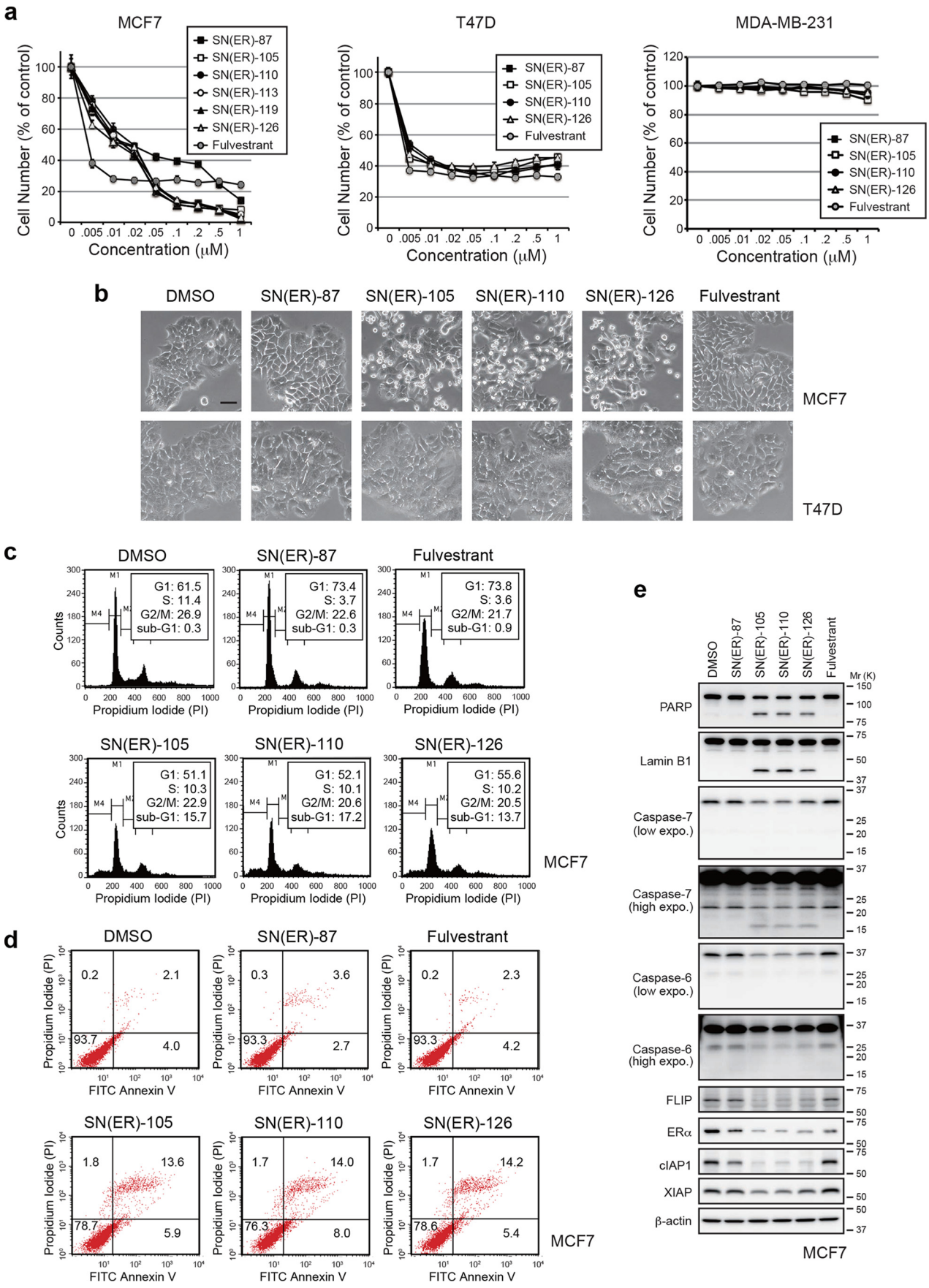
a
MCF7
T47D
MDA-MB-231
Cell Number (% of control)
Concentration (μM)
SN(ER)-87
SN(ER)-105
SN(ER)-110
SN(ER)-113
SN(ER)-119
SN(ER)-126
Fulvestrant
b
DMSO
SN(ER)-87
SN(ER)-105
SN(ER)-110
SN(ER)-126
Fulvestrant
MCF7
T47D
c
DMSO
SN(ER)-87
Fulvestrant
SN(ER)-105
SN(ER)-110
SN(ER)-126
Counts
Propidium Iodide (PI)
G1: 61.5
S: 11.4
G2/M: 26.9
sub-G1: 0.3
G1: 73.4
S: 3.7
G2/M: 22.6
sub-G1: 0.3
G1: 73.8
S: 3.6
G2/M: 21.7
sub-G1: 0.9
G1: 51.1
S: 10.3
G2/M: 22.9
sub-G1: 15.7
G1: 52.1
S: 10.1
G2/M: 20.6
sub-G1: 17.2
G1: 55.6
S: 10.2
G2/M: 20.5
sub-G1: 13.7
MCF7
d
DMSO
SN(ER)-87
Fulvestrant
SN(ER)-105
SN(ER)-110
SN(ER)-126
Propidium Iodide (PI)
FITC Annexin V
0.2
2.1
93.7
4.0
0.3
3.6
93.3
2.7
0.2
2.3
93.3
4.2
1.8
13.6
78.7
5.9
1.7
14.0
76.3
8.0
1.7
14.2
78.6
5.4
MCF7
e
DMSO
SN(ER)-87
SN(ER)-105
SN(ER)-110
SN(ER)-126
Fulvestrant
Mr (K)
PARP
Lamin B1
Caspase-7 (low expo.)
Caspase-7 (high expo.)
Caspase-6 (low expo.)
Caspase-6 (high expo.)
FLIP
ERα
cIAP1
XIAP
β-actin
MCF7

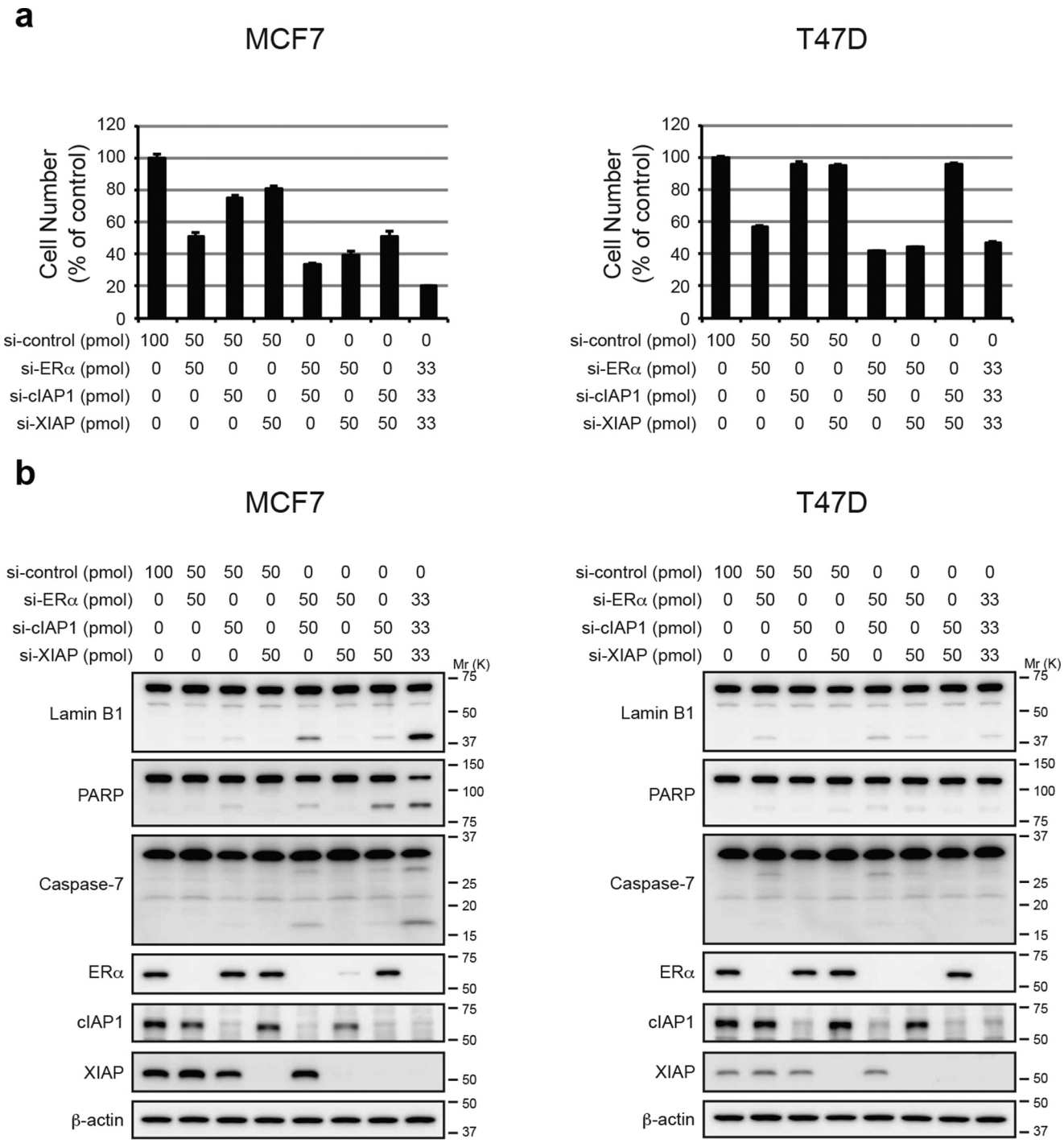

Figure 6. Depletion of IAPs induces apoptosis in MCF-7 but not T47D cells. MCF-7 or T47D cells were transfected with the indicated siRNA for 72 h. *a*, cell proliferation was evaluated by a cell viability assay. Data in the bar graph are the mean ± S.D. (*error bars*) of a experiment performed in triplicate. *b*, activation of caspases was analyzed by Western blotting. A mixture of three different siRNAs against each target was used to suppress expression.

and carefully selected SNIPER(ER)-110 and -126 as test compounds for *in vivo* comparison with SNIPER(ER)-87. When female BALB/c mice were intraperitoneally injected with SNIPER(ER)-87, -110, and -126 (30 mg/kg body weight), ERα protein levels in ovarian tissue were effectively reduced by all SNIPERs (Fig. 7*a*). To evaluate SNIPER(ER)-knockdown activities in a tumor model, we next applied MCF-7 breast tumor xenografts to nude mice. The ERα protein levels in orthotopic

Figure 5. Induction of apoptosis by SNIPER(ER)s in MCF-7 breast tumor cells. *a*, antiproliferative effects on ERα-positive human breast tumor cells by SNIPER(ER)s. Cells were treated with the indicated concentrations of SNIPER(ER)s or fulvestrant for 72 h; the remaining living cells were stained with crystal violet. *b*–*e*, SNIPER(ER)s induce apoptosis in MCF-7 cells. MCF-7 or T47D cells were treated with 100 nM SNIPER(ER)s or fulvestrant for 48 h. *b*, phase-contrast images were obtained. *Scale bars*, 50 μm. *c*, cell cycle distribution was quantified by MultiCycle software. *d*, cell death was determined by Annexin V and PI staining. *e*, activation of caspases was analyzed by Western blotting.

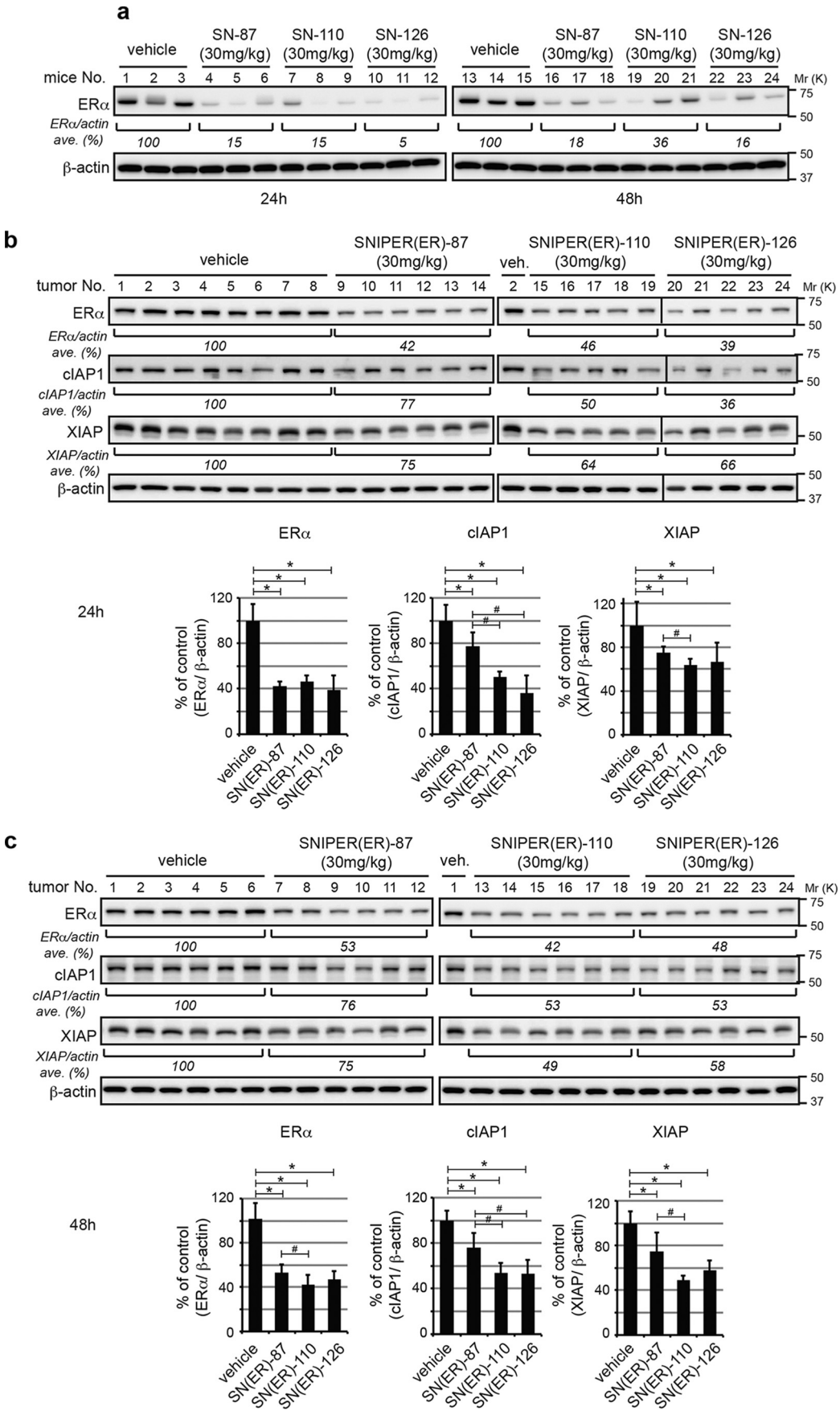
a
vehicle
SN-87 (30mg/kg)
SN-110 (30mg/kg)
SN-126 (30mg/kg)
mice No.
Mr (K)
ERα
ERα/actin ave. (%)
β-actin
24h
48h
b
SNIPER(ER)-87 (30mg/kg)
SNIPER(ER)-110 (30mg/kg)
SNIPER(ER)-126 (30mg/kg)
veh.
tumor No.
clAP1
clAP1/actin ave. (%)
XIAP
XIAP/actin ave. (%)
% of control (ERα/ β-actin)
% of control (clAP1/ β-actin)
% of control (XIAP/ β-actin)
SN(ER)-87
SN(ER)-110
SN(ER)-126
c

tumors were reduced by 40–50% in SNIPER(ER)-treated mice, compared with those in vehicle-treated mice (Fig. 7, *b* and *c*); SNIPER(ER)-110 significantly showed a significant increase in protein-knockdown activity at 48 h, compared with SNIPER(ER)-87. Treatment with SNIPER(ER)-87, -110, and -126 each reduced cIAP1 and XIAP protein levels in tumor xenografts (Fig. 7, *b* and *c*), consistent with the results of our *in vitro* analyses (Fig. 2*a*). Notably, SNIPER(ER)-110 again exhibited a significant increase in the ability to reduce cIAP1 and XIAP at 24 and 48 h, compared with SNIPER(ER)-87.

To demonstrate the therapeutic significance of these findings, we also evaluated the *in vivo* antitumor activity of SNIPER(ER)-110, compared with SNIPER(ER)-87, in an MCF-7 tumor xenograft model. When tumor-bearing mice received daily intraperitoneal injections of SNIPER(ER)-87 or SNIPER(ER)-110 (30 mg/kg body weight) for 16 days, SNIPER(ER)-110 attenuated MCF-7 tumor progression more effectively than SNIPER(ER)-87, as shown in measurements of tumor volume and tumor weight (Fig. 8, *a–c*). Notably, no obvious toxicities, including body weight changes, were observed during treatment (Fig. 8*d*). Thus, compared with SNIPER(ER)-87, SNIPER(ER)-110 showed superior antitumor activity against ERα-positive breast tumors that require IAPs for cellular survival.

Discussion

Chemical protein knockdown technologies, utilizing chimeric molecules, such as PROTACs and SNIPERs, have been recently developed to induce degradation of target proteins in cells (5–7). Our SNIPER compounds degrade cIAP1 and XIAP along with their initial target proteins, which could be advantageous in attempts to kill cancer cells because of the frequent overexpression of IAPs to suppress apoptosis in cancer cells. In this study, we developed novel SNIPER(ER)s by incorporating various IAP ligands with higher binding affinities for IAP proteins. The resulting SNIPER(ER)s (SNIPER(ER)-105, -110, and -126) each induce degradation of ERα, cIAP1, and XIAP more potently than SNIPER(ER)-87, resulting in the induction of apoptosis in MCF-7 breast tumor cells. In an *in vivo* tumor xenograft model, the novel SNIPER(ER)s exhibited activity to reduce ERα and IAPs that was respectively comparable with, and better than, that of SNIPER(ER)-87; further, the novel SNIPER(ER)-110 showed superior antitumor activity against MCF-7 tumor xenograft, compared with SNIPER(ER)-87. These results suggest that incorporating IAP ligands with higher binding affinities may be a promising strategy to develop SNIPERs with better protein knockdown and antitumor activities.

The novel SNIPER(ER)s also exhibited better protein-knockdown activity in other ERα-positive breast tumor cells, compared with SNIPER(ER)-87 (Fig. 3). However, the novel SNIPER(ER)s did not exhibit improved inhibition of growth or induction of apoptosis in T47D cells (Fig. 5), which contrasts with their activities in MCF-7 cells. We speculate that the differences in sensitivity between the two cell lines derive from differing need for IAPs, because depletion of IAPs induces apoptosis in MCF-7 cells, but not in T47D cells (Fig. 6). The role of IAPs in cancer cell survival has been suggested in many papers (32, 42–45, 58), and IAP antagonists have shown antitumor activity against many tumor cells, including breast tumor (46, 47, 59). Therefore, we hypothesize that the ability of the SNIPERs to degrade IAPs could be advantageous in treatment of cancer cells, especially those dependent on the activity of IAPs. Recently, it has been reported that the different molecular signature other than IAP frequency also specifies a sensitivity to IAP antagonists in cancer cells; the mechanism depends on autocrine release of TNFα (60–64), constitutive ubiquitylation of receptor-interacting protein kinase 1 (RIP1) (61), and expression of cellular FLICE-inhibitory protein (c-FLIP) (60) and leucine-rich repeats and immunoglobulin-like domains protein 1 (LRIG1) (65). Thus, these signatures could be used to predict sensitivity to SNIPERs as well.

Although SNIPER(ER)s induce degradation of ERα, cIAP1, and XIAP, the degradation mechanism appears different for each protein. Degradation of ERα appears to require formation of a ternary complex that is composed of ERα, SNIPER, and XIAP; we suspect this because a treatment with the individual ligand or with an structural SNIPER(ER) analog that cannot bind to IAPs does not induce degradation of ERα (13) (Fig. S5). The pharmacological hook effect that is observed during SNIPER(ER)-induced ERα degradation further supports the hypothesis that ternary complex formation is required (13). In contrast, the degradation of cIAP1 is triggered by binding of the IAP antagonist module to the BIR3 domain of cIAP1, thus inducing autoubiquitylation. In this case, the ternary complex is not required, and no hook effect is observed (13). Notably, the degradation mechanism of XIAP remains ambiguous. Degradation of XIAP was induced by SNIPER(ER)s but not by IAP antagonists nor by the mixture of IAP antagonist and 4-hydroxytamoxifen (Fig. S5), suggesting that the ternary complex is required for XIAP degradation. Consistent with this hypothesis, XIAP degradation by SNIPER(ER)-87 was not observed in the ERα-negative MDA-MB-231 breast cancer cells (Fig. S5). Thus, XIAP degradation seems to require the same ternary complex formation that is required for ERα degradation. However, XIAP degradation requires more time and is inefficient, compared with degradation of the ERα target protein (Figs. 2*a* and 3). It is likely that part of the population of XIAP in the ternary complex is subjected to ubiquitylation and proteasomal degradation. Because XIAP degradation was more prominently observed in T47D cells than in MCF-7 and ZR-75-1 cells, we

Figure 7. *In vivo* protein knockdown by SNIPER(ER)s in mice. *a*, *in vivo* protein knockdown in ovarian tissue. Female BALB/c mice were injected with vehicle or 30 mg/kg SNIPER(ER)s. After 24 or 48 h, the mice were sacrificed, and their ovaries were collected and analyzed by Western blotting with the indicated antibodies. *Numbers below* the *ERα panel* represent the ERα/actin ratio, normalized by designating the expression from the vehicle control condition as 100% (average of each group). *b* and *c*, MCF-7 human breast tumor cells were inoculated into mammary fat pads of 6-week-old female BALB/c nude mice. The tumor-bearing mice were intraperitoneally injected with SNIPER(ER)s. After 24 or 48 h, mice were sacrificed, and ERα protein levels in tumor xenografts were analyzed by Western blotting. *Bar graphs* represent the mean ± S.D. (*error bars*) of each group. *, $p < 0.05$ in two-tailed Student's *t* test compared with vehicle control. #, $p < 0.05$ in two-tailed Student's *t* test compared with SNIPER(ER)-87.

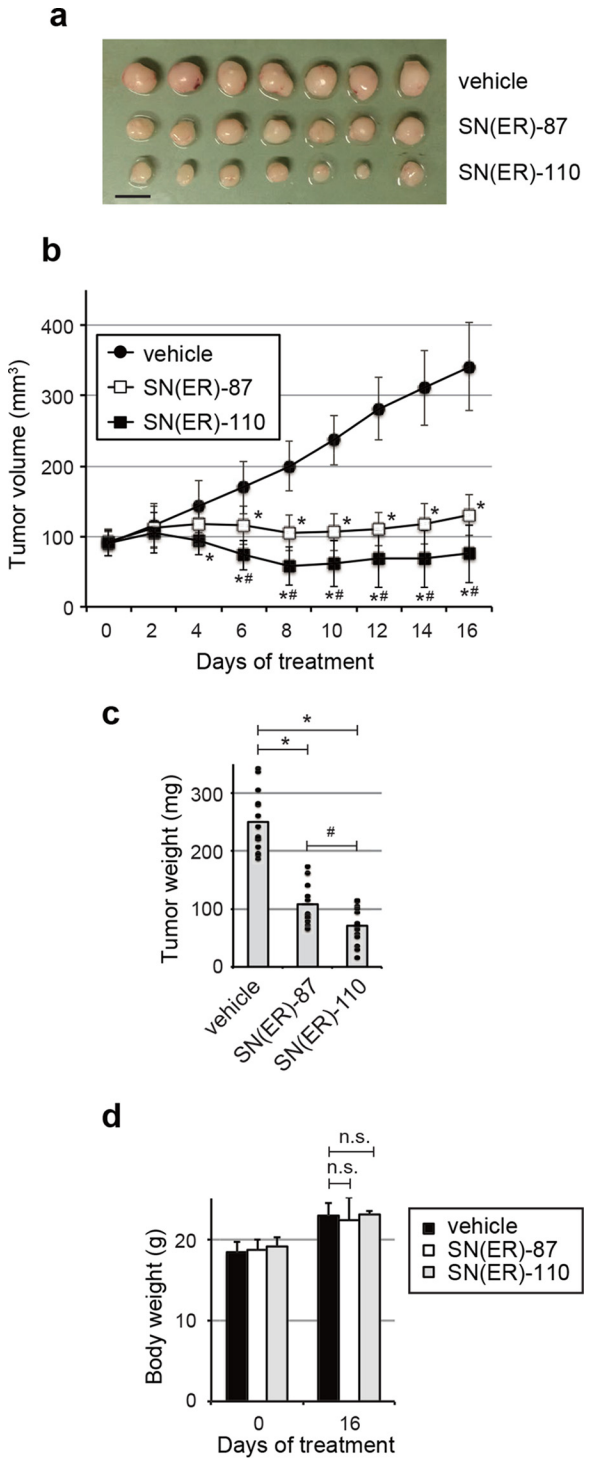

Figure 8. Antitumor activity of SNIPER(ER)s. Growth inhibition by SNIPER(ER)s of MCF-7 orthotopic breast tumor xenografts in nude mice. *a*, representative tumors. *Scale bar*, 10 mm. The tumor volume (*b*) or weight (*c*) represents the mean ± S.D. (*error bars*) of each group (mice, $n = 7$ each; tumors, $n = 14$ each; *, $p < 0.05$ in two-tailed Student's *t* test compared with vehicle; #, $p < 0.05$ in two-tailed Student's *t* test compared with SNIPER(ER)-87). Mice were administered vehicle or SNIPER(ER)s (30 mg/kg) intraperitoneally, every 24 h. *d*, treatment with SNIPER(ER)s did not induce significant body weight loss in mice after 16 days.

measured the expression of ERα, cIAP1, and XIAP in these cells (Fig. S6). We found that the ratio of XIAP to ERα is one-third and one-thirteenth less in T47D cells than in MCF-7 cells and in XR-75-1 cells, respectively, suggesting that the lower expression of XIAP may increase the significance of its degradation in T47D cells. Thus, although the degradation mechanisms differ, SNIPER(ER)s induce degradation of ERα, cIAP1, and XIAP, culminating in an anti-tumor effect that is directed against breast cancer cells.

It has been reported that ERα translocates from the cytosol to the nucleus upon binding with tamoxifen (66, 67). This is also observed after treatment with SNIPER(ER)s, because the relative amount of ERα increased in the nucleus, compared with the cytosol, upon treatment with SNIPER(ER)s; this was more clearly observed in the presence of MG132 (Fig. S7, *a* and *b*). Interestingly, the amount of XIAP increased in the nucleus upon treatment with SNIPER(ER)s; this was also more clearly observed in the presence of MG132. These results suggest that when a SNIPER(ER) penetrates a cell, it induces formation of the ternary complex composed of ERα, SNIPER(ER), and XIAP in the cytosol; ERα then translocates to the nucleus together with the bound XIAP. Thus, in the presence of SNIPER(ER), ERα interacts with XIAP sufficiently to tether XIAP in the nucleus, consistent with the preferential recruitment of XIAP, but not cIAP1, to ERα.

In summary, we have developed potent SNIPER(ER)s by incorporation of high-affinity IAP ligands. These SNIPER(ER)s induce degradation of ERα and IAPs and exhibit antitumor activity against breast tumors that require IAPs for survival. These IAP ligand modules could be utilized to develop novel SNIPERs with activity against various oncogenic proteins and enhanced antitumor capabilities.

Experimental procedures

Chemistry

Chemical synthesis and physicochemical data for SNIPER compounds are provided in the supporting information.

Cell culture

Human breast carcinoma MCF-7, T47D, and ZR-75-1 cells were maintained in RPMI 1640 medium containing 10% fetal bovine serum (FBS) and 100 μg/ml kanamycin. Human breast carcinoma MDA-MB-231 cells were maintained in Dulbecco's modified Eagle's medium containing 10% FBS and 100 μg/ml kanamycin. All of the cell lines were purchased from ATCC (Manassas, VA), and their cell authentications were confirmed by morphology, karyotyping, and PCR-based approaches in ATCC. Cells were treated with various concentrations of SNIPER compounds for the indicated times.

Western blotting

Cells were lysed with SDS lysis buffer (0.1 M Tris-HCl, pH 8.0, 10% glycerol, 1% SDS) and immediately boiled for 10 min to obtain clear lysates. Nuclear and cytoplasmic extracts were prepared with NE-PER nuclear and cytoplasmic extraction reagents (Thermo Fisher Scientific). Protein concentration was measured by the BCA method (Pierce); lysates containing equal amounts of proteins were separated by SDS-PAGE and transferred to polyvinylidene difluoride membranes (Millipore, Darmstadt, Germany) for Western blot analysis using the

appropriate antibodies. Immunoreactive proteins were visualized using the Immobilon Western chemiluminescent HRP substrate (Millipore) or Clarity Western ECL substrate (Bio-Rad); light emission intensity was quantified using an LAS-3000 lumino-image analyzer equipped with Image Gauge version 2.3 software (Fuji, Tokyo, Japan). The antibodies used in this study were as follows: anti-ERα rabbit monoclonal antibody (mAb) (Cell Signaling Technology (Danvers, MA), 8644), anti-ERα rabbit polyclonal antibody (pAb) (Santa Cruz Biotechnology, Inc. (Dallas, TX), sc-542 and sc-543), anti-cIAP1 goat pAb (R&D Systems (Minneapolis, MN), AF8181), anti-cIAP1 rat mAb (Enzo Life Sciences (Farmingdale, NY), 1E1-1-10), anti-β-actin mouse mAb (Sigma, A5316), anti-XIAP rabbit pAb (Cell Signaling Technology, 2042), anti-GAPDH rabbit pAb (Santa Cruz Biotechnology, sc-25778), anti-lamin B1 goat pAb (Santa Cruz Biotechnology, sc-6216), anti-histone H3 goat pAb (Santa Cruz Biotechnology, sc-8654), anti-PARP rabbit pAb (Cell Signaling Technology, 9542), anti-caspase-6 rabbit pAb (Cell Signaling Technology, 9762), anti-caspase-7 rabbit mAb (Cell Signaling Technology, 12827).

Measurement of binding affinities of ERα and IAPs

The bindings between test compounds and cIAP1, cIAP2, or XIAP were determined by a time-resolved FRET assay using His-IAP proteins (XIAP, cIAP1, or cIAP2), FITC-Smac, Tb-SA, and biotinylated anti-His antibody, as described previously (14).

The binding between test compounds and the human ERα protein was determined using the PolarScreen™ Estrogen Receptor-α Competitor Assay Green (Thermo Fisher Scientific, A15882) containing recombinant ERα full-length protein, Fluormone ES2 Green2, and ES2 screening buffer. Purified ERα and Fluormone ES2 were diluted with assay buffer to final concentrations of 25 and 4.5 nM, respectively, and 4 μl of each dilution was added to each well of a 384-well black low-volume assay plate (Greiner, 784076). Then 2 μl of the ES2 screening buffer, containing test compounds or DMSO, was added to the well. The plate was subjected to centrifugation and incubated at room temperature for 1 h; then the intensity of the fluorescence polarization signal was measured by a plate reader (Envision, PerkinElmer Life Sciences). Wells containing ERα and Fluormone ES2 were used as a positive control, and wells containing only Fluormone ES2 were used as a negative control. IC_{50} values and 95% confidence interval were calculated by XLfit (ID Business Solutions, fit model 204) from the data expressed as percentage of control inhibition.

Immunoprecipitation

MCF-7 or T47D cells were treated with the indicated concentrations of the indicated compounds, in combination with 10 μM MG132, for 3 h. Cells were lysed using immunoprecipitation lysis buffer (10 mM Hepes, pH 7.4, 142.5 mM KCl, 5 mM $MgCl_2$, 1 mM EGTA, and 0.1% Triton X-100), containing protease inhibitor mixtures, rotated for 15 min at 4 °C, and centrifuged at 15,000 rpm for 10 min at 4 °C to obtain the supernatants. Lysates that had been precleared with naked protein G-Sepharose were immunoprecipitated with protein G-Sepharose beads that were preincubated with anti-ERα rabbit pAb (Santa Cruz Biotechnology, sc-543) for 2 h at 4 °C. The precipitates were washed with immunoprecipitation lysis buffer four times and analyzed by Western blotting.

siRNA transfection

MCF-7 or T47D cells were transiently transfected with a gene-specific siRNA or a negative control siRNA (Qiagen, Valencia, CA) using Lipofectamine RNAi MAX reagent (Life Technologies, Inc.). The siRNA sequences used in this study were as follows: human ERα-1 (5′-CGACAUGCUGCUGGCUACAUCAUCU-3′), ERα-2 (5′-UCACAGACACUUUGAUCCACCUGAU-3′), ERα-3 (5′-GACCGAAGAGGAGGGAGAAUGUUGA-3′), cIAP1–1 (5′-UCUAGAGCAGUUGAAGACAUCUCUU-3′), cIAP1-2 (5′-GCUGUAGCUUUAUUCAGAAUCUGGU-3′), cIAP1–3 (5′-GGAAAUGCUGCGGCCAACAUCUUCA-3′), XIAP-1 (5′-ACACUGGCACGAGCAGGGUUUCUUU-3′), XIAP-2 (5′-GAAGGAGAUACCGUGCGGUGCUUUA-3′), and XIAP-3 (5′-CCAGAAUGGUCAGUACAAAGUUGAA-3′).

Cell viability assay

Cell viability was evaluated by crystal violet staining. Cells were treated with graded concentrations of the SNIPER compounds for 72 h and then stained with 0.1% crystal violet (Wako, Osaka, Japan) in 1% ethanol for 15 min at room temperature. Cells were rinsed thoroughly with distilled water and then lysed in 1% SDS. The absorbance of the cell lysate at 600 nm was measured using an EnVision multilabel plate reader (PerkinElmer Life Sciences).

In vivo protein knockdown

All procedures of the animal experiments were reviewed and approved by the Institutional Animal Experiment Review Committee of the National Institute of Health Sciences (NIHS), and those experiments were conducted in accordance with the guidelines approved by the Care and Use of Animals published by the Institutional Animal Ethical Committee. Mice were housed in pathogen-free animal facilities at the NIHS with 12-h light/dark cycles and were fed rodent chow and water *ad libitum*. For Fig. 7*a*, female 6-week-old BALB/c mice (Clea Japan, Tokyo, Japan) were randomized and divided into eight treatment groups ($n = 3$) and then treated with vehicle or 30 mg/kg SNIPER(ER)s for 24 h or 48 h. For Fig. 7 (*b* and *c*), each suspension of 1×10^7 MCF-7 cells was mixed with an equal volume of Matrigel (Corning Inc.) and injected (100 μl total) into the left and right mammary fat pads of 6-week-old female BALB/c nude mice (Clea Japan). After cell inoculation, β-estradiol solution was subcutaneously injected into the neck twice at intervals of 6 days. Fourteen days after the last β-estradiol injection, tumor-bearing mice were randomized and divided into two or three treatment groups as follows: for Fig. 7*b*: 1) vehicle treatment for 24 h ($n = 3$), 2) 30 mg/kg SNIPER(ER)-87 treatment for 24 h ($n = 2$), 3) 30 mg/kg SNIPER(ER)-110 treatment for 24 h ($n = 2$), and 4) 30 mg/kg SNIPER(ER)-126 treatment for 24 h ($n = 2$); for Fig. 7*c*: 1) vehicle treatment for 48 h ($n = 3$), 2) 30 mg/kg SNIPER(ER)-87 treatment for 48 h ($n = 3$), 3) 30 mg/kg SNIPER(ER)-110 treatment for 48 h ($n = 3$), and 4) 30 mg/kg SNIPER(ER)-126 treatment for 48 h ($n = 3$). Com-

pounds were administered via intraperitoneal injection. After the indicated treatment periods, the mice were sacrificed, and tissues were excised. Total lysates from the ovaries and tumors were analyzed by Western blotting.

In vivo tumor growth inhibition

Each suspension of 1×10^7 MCF-7 cells was mixed with an equal volume of Matrigel (BD Biosciences) and inoculated (100 μl total) into the left and right mammary fat pads of 6-week-old female BALB/c nude mice (Clea Japan) that had received an β-estradiol pellet (6 μg/day) (Innovative Research of America, Sarasota, FL) under the neck skin. After 4 days, mice bearing tumors of $\sim$100 mm^3 in size were randomized and divided into two groups ($n = 7$). One group served as a control for the dosing vehicle; the other groups were administered SNIPER(ER)-87 or SNIPER(ER)-110 (30 mg/kg, intraperitoneally, every 24 h), respectively. Tumor volumes were measured every 2 days using a caliper and calculated according to the standard formula: (length $\times$ width^2)/2. At 16 days, mice were sacrificed, and the tumors were weighed and excised.

Cell cycle analysis

After treatment, cells were gently trypsinized and washed with serum-containing medium. Cells were collected by centrifugation and then washed with PBS and fixed in 70% ice-cold ethanol for 1 h on ice. The cells were then washed, treated with 1 mg/ml RNase A for 1 h at 37 °C, and stained in PI solution (50 μg/ml in 0.1% sodium citrate, 0.1% NP-40). The stained cells were analyzed in a FACScan flow cytometer (BD Biosciences).

Measurement of apoptosis by flow cytometer

Apoptosis was analyzed with an annexin V-FITC apoptosis detection kit (BioVision). After treatment, cells were gently trypsinized and washed with serum-containing medium. Cells were collected by centrifugation and then washed with PBS and resuspended in binding buffer. The cells were stained with annexin V-FITC and PI at room temperature for 5 min in the dark, according to the manufacturer's instructions, and analyzed in a FACScan flow cytometer (BD Biosciences).

Statistical analysis

Student's t test was used to evaluate differences among the experimental groups. Values of $p < 0.05$ were considered significant.

Author contributions—N. O. and M. N. designed the experiments; Y. M., K. N., K. S., I. F., M. I., Y. H., Y. I., H. N., and N. C. designed and synthesized the compounds; N. O., K. O., N. S., T. H., T. S., O. S., and R. K. performed the experiments and analyzed the data; N. O., K. S., O. U., H. N., and M. N. wrote the manuscript; and M. N. supervised all research. All authors discussed and checked the manuscript.

Acknowledgments—We thank Mariko Seki for measurement of the protein-knockdown activities and Ryan Chastain-Gross, Ph.D. (Edanz Group) for editing a draft of the manuscript.

References

1. Wells, J. A., and McClendon, C. L. (2007) Reaching for high-hanging fruit in drug discovery at protein-protein interfaces. *Nature* **450,** 1001–1009 CrossRef Medline
2. Arkin, M. R., and Wells, J. A. (2004) Small-molecule inhibitors of protein-protein interactions: progressing towards the dream. *Nat. Rev. Drug Discov.* **3,** 301–317 CrossRef Medline
3. Mansoori, B., Sandoghchian Shotorbani, S., and Baradaran, B. (2014) RNA interference and its role in cancer therapy. *Adv. Pharm. Bull.* **4,** 313–321 Medline
4. Ozcan, G., Ozpolat, B., Coleman, R. L., Sood, A. K., and Lopez-Berestein, G. (2015) Preclinical and clinical development of siRNA-based therapeutics. *Adv. Drug Deliv. Rev.* **87,** 108–119 CrossRef Medline
5. Ohoka, N., Shibata, N., Hattori, T., and Naito, M. (2016) Protein knockdown technology: application of ubiquitin ligase to cancer therapy. *Curr. Cancer Drug Targets* **16,** 136–146 CrossRef Medline
6. Toure, M., and Crews, C. M. (2016) Small-molecule PROTACS: new approaches to protein degradation. *Angew. Chem. Int. Ed. Engl.* **55,** 1966–1973 CrossRef Medline
7. Lai, A. C., and Crews, C. M. (2017) Induced protein degradation: an emerging drug discovery paradigm. *Nat. Rev. Drug Discov.* **16,** 101–114 CrossRef Medline
8. Bondeson, D. P., Mares, A., Smith, I. E., Ko, E., Campos, S., Miah, A. H., Mulholland, K. E., Routly, N., Buckley, D. L., Gustafson, J. L., Zinn, N., Grandi, P., Shimamura, S., Bergamini, G., Faelth-Savitski, M., *et al.* (2015) Catalytic in vivo protein knockdown by small-molecule PROTACs. *Nat. Chem. Biol.* **11,** 611–617 CrossRef Medline
9. Lu, J., Qian, Y., Altieri, M., Dong, H., Wang, J., Raina, K., Hines, J., Winkler, J. D., Crew, A. P., Coleman, K., and Crews, C. M. (2015) Hijacking the E3 ubiquitin ligase cereblon to efficiently target BRD4. *Chem. Biol.* **22,** 755–763 CrossRef Medline
10. Winter, G. E., Buckley, D. L., Paulk, J., Roberts, J. M., Souza, A., Dhe-Paganon, S., and Bradner, J. E. (2015) Drug Development: phthalimide conjugation as a strategy for *in vivo* target protein degradation. *Science* **348,** 1376–1381 CrossRef Medline
11. Soares, P., Gadd, M. S., Frost, J., Galdeano, C., Ellis, L., Epemolu, O., Rocha, S., Read, K. D., and Ciulli, A. (2018) Group-based optimization of potent and cell-active inhibitors of the von Hippel-Lindau (VHL) E3 ubiquitin ligase: structure-activity relationships leading to the chemical probe (2*S*,4*R*)-1-((*S*)-2-(1-cyanocyclopropanecarboxamido)-3,3-dimethylbutanoyl)-4-hydroxy-*N*-(4-(4-methylthiazol-5-yl)benzyl)pyrrolidine-2-carboxamide (VH298). *J. Med. Chem.* **61,** 599–618 CrossRef Medline
12. Itoh, Y., Ishikawa, M., Naito, M., and Hashimoto, Y. (2010) Protein knockdown using methyl bestatin-ligand hybrid molecules: design and synthesis of inducers of ubiquitination-mediated degradation of cellular retinoic acid-binding proteins. *J. Am. Chem. Soc.* **132,** 5820–5826 CrossRef Medline
13. Ohoka, N., Okuhira, K., Ito, M., Nagai, K., Shibata, N., Hattori, T., Ujikawa, O., Shimokawa, K., Sano, O., Koyama, R., Fujita, H., Teratani, M., Matsumoto, H., Imaeda, Y., Nara, H., *et al.* (2017) *In vivo* knockdown of pathogenic proteins via specific and nongenetic inhibitor of apoptosis protein (IAP)-dependent protein erasers (SNIPERs). *J. Biol. Chem.* **292,** 4556–4570 CrossRef Medline
14. Shibata, N., Miyamoto, N., Nagai, K., Shimokawa, K., Sameshima, T., Ohoka, N., Hattori, T., Imaeda, Y., Nara, H., Cho, N., and Naito, M. (2017) Development of protein degradation inducers of oncogenic BCR-ABL protein by conjugation of ABL kinase inhibitors and IAP ligands. *Cancer Sci.* **108,** 1657–1666 CrossRef Medline
15. Shimokawa, K., Shibata, N., Sameshima, T., Miyamoto, N., Ujikawa, O., Nara, H., Ohoka, N., Hattori, T., Cho, N., and Naito, M. (2017) Targeting the allosteric site of oncoprotein BCR-ABL as an alternative strategy for effective target protein degradation. *ACS Med. Chem. Lett.* **8,** 1042–1047 CrossRef Medline
16. Ohoka, N., Nagai, K., Shibata, N., Hattori, T., Nara, H., Cho, N., and Naito, M. (2017) SNIPER(TACC3) induces cytoplasmic vacuolization and sensitizes cancer cells to Bortezomib. *Cancer Sci.* **108,** 1032–1041 CrossRef Medline

17. Okuhira, K., Ohoka, N., Sai, K., Nishimaki-Mogami, T., Itoh, Y., Ishikawa, M., Hashimoto, Y., and Naito, M. (2011) Specific degradation of CRABP-II via cIAP1-mediated ubiquitylation induced by hybrid molecules that crosslink cIAP1 and the target protein. *FEBS Lett.* **585,** 1147–1152 CrossRef Medline
18. Okuhira, K., Demizu, Y., Hattori, T., Ohoka, N., Shibata, N., Nishimaki-Mogami, T., Okuda, H., Kurihara, M., and Naito, M. (2013) Development of hybrid small molecules that induce degradation of estrogen receptor-α and necrotic cell death in breast cancer cells. *Cancer Sci.* **104,** 1492–1498 CrossRef Medline
19. Demizu, Y., Ohoka, N., Nagakubo, T., Yamashita, H., Misawa, T., Okuhira, K., Naito, M., and Kurihara, M. (2016) Development of a peptide-based inducer of nuclear receptors degradation. *Bioorg. Med. Chem. Lett.* **26,** 2655–2658 CrossRef Medline
20. Ohoka, N., Misawa, T., Kurihara, M., Demizu, Y., and Naito, M. (2017) Development of a peptide-based inducer of protein degradation targeting NOTCH1. *Bioorg. Med. Chem. Lett.* **27,** 4985–4988 CrossRef Medline
21. Sun, B., Fiskus, W., Qian, Y., Rajapakshe, K., Raina, K., Coleman, K. G., Crew, A. P., Shen, A., Saenz, D. T., Mill, C. P., Nowak, A. J., Jain, N., Zhang, L., Wang, M., Khoury, J. D., *et al.* (2018) BET protein proteolysis targeting chimera (PROTAC) exerts potent lethal activity against mantle cell lymphoma cells. *Leukemia* **32,** 343–352 CrossRef Medline
22. Remillard, D., Buckley, D. L., Paulk, J., Brien, G. L., Sonnett, M., Seo, H. S., Dastjerdi, S., Wühr, M., Dhe-Paganon, S., Armstrong, S. A., and Bradner, J. E. (2017) Degradation of the BAF complex factor BRD9 by heterobifunctional ligands. *Angew. Chem. Int. Ed. Engl.* **56,** 5738–5743 CrossRef Medline
23. Winter, G. E., Mayer, A., Buckley, D. L., Erb, M. A., Roderick, J. E., Vittori, S., Reyes, J. M., di Iulio, J., Souza, A., Ott, C. J., Roberts, J. M., Zeid, R., Scott, T. G., Paulk, J., Lachance, K., *et al.* (2017) BET bromodomain proteins function as master transcription elongation factors independent of CDK9 recruitment. *Mol. Cell* **67,** 5–18.e19 CrossRef Medline
24. Schiedel, M., Herp, D., Hammelmann, S., Swyter, S., Lehotzky, A., Robaa, D., Oláh, J., Ovádi, J., Sippl, W., and Jung, M. (2018) Chemically induced degradation of sirtuin 2 (Sirt2) by a proteolysis targeting chimera (PROTAC) based on sirtuin rearranging ligands (SirReals). *J. Med. Chem.* **61,** 482–491 CrossRef Medline
25. Zhou, B., Hu, J., Xu, F., Chen, Z., Bai, L., Fernandez-Salas, E., Lin, M., Liu, L., Yang, C. Y., Zhao, Y., McEachern, D., Przybranowski, S., Wen, B., Sun, D., and Wang, S. (2018) Discovery of a small-molecule degrader of bromodomain and extra-terminal (BET) proteins with picomolar cellular potencies and capable of achieving tumor regression. *J. Med. Chem.* **61,** 462–481 CrossRef Medline
26. Crew, A. P., Raina, K., Dong, H., Qian, Y., Wang, J., Vigil, D., Serebrenik, Y. V., Hamman, B. D., Morgan, A., Ferraro, C., Siu, K., Neklesa, T. K., Winkler, J. D., Coleman, K. G., and Crews, C. M. (2018) Identification and characterization of Von Hippel-Lindau-recruiting proteolysis targeting chimeras (PROTACs) of TANK-binding kinase. *J. Med. Chem.* **61,** 583–598 CrossRef Medline
27. Ohoka, N., Nagai, K., Hattori, T., Okuhira, K., Shibata, N., Cho, N., and Naito, M. (2014) Cancer cell death induced by novel small molecules degrading the TACC3 protein via the ubiquitin-proteasome pathway. *Cell Death Dis.* **5,** e1513 CrossRef Medline
28. Shibata, N., Nagai, K., Morita, Y., Ujikawa, O., Ohoka, N., Hattori, T., Koyama, R., Sano, O., Imaeda, Y., Nara, H., Cho, N., and Naito, M. (2018) Development of protein degradation inducers of androgen receptor by conjugation of androgen receptor ligands and inhibitor of apoptosis protein ligands. *J. Med. Chem.* **61,** 543–575 CrossRef Medline
29. Chan, K. H., Zengerle, M., Testa, A., and Ciulli, A. (2018) Impact of target warhead and linkage vector on inducing protein degradation: comparison of bromodomain and extra-terminal (BET) degraders derived from triazolodiazepine (JQ1) and tetrahydroquinoline (I-BET726) BET inhibitor scaffolds. *J. Med. Chem.* **61,** 504–513 CrossRef Medline
30. Lai, A. C., Toure, M., Hellerschmied, D., Salami, J., Jaime-Figueroa, S., Ko, E., Hines, J., and Crews, C. M. (2016) Modular PROTAC design for the degradation of oncogenic BCR-ABL. *Angew. Chem. Int. Ed. Engl.* **55,** 807–810 CrossRef Medline
31. Raina, K., Lu, J., Qian, Y., Altieri, M., Gordon, D., Rossi, A. M., Wang, J., Chen, X., Dong, H., Siu, K., Winkler, J. D., Crew, A. P., Crews, C. M., and Coleman, K. G. (2016) PROTAC-induced BET protein degradation as a therapy for castration-resistant prostate cancer. *Proc. Natl. Acad. Sci. U.S.A.* **113,** 7124–7129 CrossRef Medline
32. Fulda, S., and Vucic, D. (2012) Targeting IAP proteins for therapeutic intervention in cancer. *Nat. Rev. Drug Discov.* **11,** 109–124 CrossRef Medline
33. Deveraux, Q. L., and Reed, J. C. (1999) IAP family proteins: suppressors of apoptosis. *Genes Dev.* **13,** 239–252 CrossRef Medline
34. Salvesen, G. S., and Duckett, C. S. (2002) IAP proteins: blocking the road to death's door. *Nat. Rev. Mol. Cell Biol.* **3,** 401–410 CrossRef Medline
35. Deveraux, Q. L., Takahashi, R., Salvesen, G. S., and Reed, J. C. (1997) X-linked IAP is a direct inhibitor of cell-death proteases. *Nature* **388,** 300–304 CrossRef Medline
36. Hao, Y., Sekine, K., Kawabata, A., Nakamura, H., Ishioka, T., Ohata, H., Katayama, R., Hashimoto, C., Zhang, X., Noda, T., Tsuruo, T., and Naito, M. (2004) Apollon ubiquitinates SMAC and caspase-9, and has an essential cytoprotection function. *Nat. Cell Biol.* **6,** 849–860 CrossRef Medline
37. Suzuki, Y., Nakabayashi, Y., and Takahashi, R. (2001) Ubiquitin-protein ligase activity of X-linked inhibitor of apoptosis protein promotes proteasomal degradation of caspase-3 and enhances its anti-apoptotic effect in Fas-induced cell death. *Proc. Natl. Acad. Sci. U.S.A.* **98,** 8662–8667 CrossRef Medline
38. Kikuchi, R., Ohata, H., Ohoka, N., Kawabata, A., and Naito, M. (2014) APOLLON protein promotes early mitotic CYCLIN A degradation independent of the spindle assembly checkpoint. *J. Biol. Chem.* **289,** 3457–3467 CrossRef Medline
39. Imoto, I., Tsuda, H., Hirasawa, A., Miura, M., Sakamoto, M., Hirohashi, S., and Inazawa, J. (2002) Expression of cIAP1, a target for 11q22 amplification, correlates with resistance of cervical cancers to radiotherapy. *Cancer Res.* **62,** 4860–4866 Medline
40. Imoto, I., Yang, Z. Q., Pimkhaokham, A., Tsuda, H., Shimada, Y., Imamura, M., Ohki, M., and Inazawa, J. (2001) Identification of cIAP1 as a candidate target gene within an amplicon at 11q22 in esophageal squamous cell carcinomas. *Cancer Res.* **61,** 6629–6634 Medline
41. Tamm, I., Kornblau, S. M., Segall, H., Krajewski, S., Welsh, K., Kitada, S., Scudiero, D. A., Tudor, G., Qui, Y. H., Monks, A., Andreeff, M., and Reed, J. C. (2000) Expression and prognostic significance of IAP-family genes in human cancers and myeloid leukemias. *Clin. Cancer Res.* **6,** 1796–1803 Medline
42. Jaffer, S., Orta, L., Sunkara, S., Sabo, E., and Burstein, D. E. (2007) Immunohistochemical detection of antiapoptotic protein X-linked inhibitor of apoptosis in mammary carcinoma. *Hum. Pathol.* **38,** 864–870 CrossRef Medline
43. Wang, J., Liu, Y., Ji, R., Gu, Q., Zhao, X., Liu, Y., and Sun, B. (2010) Prognostic value of the X-linked inhibitor of apoptosis protein for invasive ductal breast cancer with triple-negative phenotype. *Hum. Pathol.* **41,** 1186–1195 CrossRef Medline
44. Foster, F. M., Owens, T. W., Tanianis-Hughes, J., Clarke, R. B., Brennan, K., Bundred, N. J., and Streuli, C. H. (2009) Targeting inhibitor of apoptosis proteins in combination with ErbB antagonists in breast cancer. *Breast Cancer Res.* **11,** R41 CrossRef Medline
45. Yang, L., Cao, Z., Yan, H., and Wood, W. C. (2003) Coexistence of high levels of apoptotic signaling and inhibitor of apoptosis proteins in human tumor cells: implication for cancer specific therapy. *Cancer Res.* **63,** 6815–6824 Medline
46. Cohen, P., and Tcherpakov, M. (2010) Will the ubiquitin system furnish as many drug targets as protein kinases? *Cell* **143,** 686–693 CrossRef Medline
47. Wang, S., Bai, L., Lu, J., Liu, L., Yang, C. Y., and Sun, H. (2012) Targeting inhibitors of apoptosis proteins (IAPs) for new breast cancer therapeutics. *J. Mammary Gland Biol. Neoplasia* **17,** 217–228 CrossRef Medline
48. Varfolomeev, E., Blankenship, J. W., Wayson, S. M., Fedorova, A. V., Kayagaki, N., Garg, P., Zobel, K., Dynek, J. N., Elliott, L. O., Wallweber, H. J., Flygare, J. A., Fairbrother, W. J., Deshayes, K., Dixit, V. M., and Vucic, D. (2007) IAP antagonists induce autoubiquitination of c-IAPs, NF-κB acti-

vation, and TNFα-dependent apoptosis. *Cell* **131,** 669–681 CrossRef Medline

49. Vince, J. E., Wong, W. W., Khan, N., Feltham, R., Chau, D., Ahmed, A. U., Benetatos, C. A., Chunduru, S. K., Condon, S. M., McKinlay, M., Brink, R., Leverkus, M., Tergaonkar, V., Schneider, P., Callus, B. A., *et al.* (2007) IAP antagonists target cIAP1 to induce TNFα-dependent apoptosis. *Cell* **131,** 682–693 CrossRef Medline
50. Bertrand, M. J., Milutinovic, S., Dickson, K. M., Ho, W. C., Boudreault, A., Durkin, J., Gillard, J. W., Jaquith, J. B., Morris, S. J., and Barker, P. A. (2008) cIAP1 and cIAP2 facilitate cancer cell survival by functioning as E3 ligases that promote RIP1 ubiquitination. *Mol. Cell* **30,** 689–700 CrossRef Medline
51. Sekine, K., Takubo, K., Kikuchi, R., Nishimoto, M., Kitagawa, M., Abe, F., Nishikawa, K., Tsuruo, T., and Naito, M. (2008) Small molecules destabilize cIAP1 by activating auto-ubiquitylation. *J. Biol. Chem.* **283,** 8961–8968 CrossRef Medline
52. Oost, T. K., Sun, C., Armstrong, R. C., Al-Assaad, A. S., Betz, S. F., Deckwerth, T. L., Ding, H., Elmore, S. W., Meadows, R. P., Olejniczak, E. T., Oleksijew, A., Oltersdorf, T., Rosenberg, S. H., Shoemaker, A. R., Tomaselli, K. J., Zou, H., and Fesik, S. W. (2004) Discovery of potent antagonists of the antiapoptotic protein XIAP for the treatment of cancer. *J. Med. Chem.* **47,** 4417–4426 CrossRef Medline
53. Hennessy, E. J., Saeh, J. C., Sha, L., MacIntyre, T., Wang, H., Larsen, N. A., Aquila, B. M., Ferguson, A. D., Laing, N. M., and Omer, C. A. (2012) Discovery of aminopiperidine-based Smac mimetics as IAP antagonists. *Bioorg. Med. Chem. Lett.* **22,** 1690–1694 CrossRef Medline
54. Cohen, F., Koehler, M. F., Bergeron, P., Elliott, L. O., Flygare, J. A., Franklin, M. C., Gazzard, L., Keteltas, S. F., Lau, K., Ly, C. Q., Tsui, V., and Fairbrother, W. J. (2010) Antagonists of inhibitor of apoptosis proteins based on thiazole amide isosteres. *Bioorg. Med. Chem. Lett.* **20,** 2229–2233 CrossRef Medline
55. Flygare, J. A., Beresini, M., Budha, N., Chan, H., Chan, I. T., Cheeti, S., Cohen, F., Deshayes, K., Doerner, K., Eckhardt, S. G., Elliott, L. O., Feng, B., Franklin, M. C., Reisner, S. F., Gazzard, L., *et al.* (2012) Discovery of a potent small-molecule antagonist of inhibitor of apoptosis (IAP) proteins and clinical candidate for the treatment of cancer (GDC-0152). *J. Med. Chem.* **55,** 4101–4113 CrossRef Medline
56. Hall, J. M., and McDonnell, D. P. (2005) Coregulators in nuclear estrogen receptor action: from concept to therapeutic targeting. *Mol. Interv.* **5,** 343–357 CrossRef Medline
57. Nadji, M., Gomez-Fernandez, C., Ganjei-Azar, P., and Morales, A. R. (2005) Immunohistochemistry of estrogen and progesterone receptors reconsidered: experience with 5,993 breast cancers. *Am. J. Clin. Pathol.* **123,** 21–27 CrossRef Medline
58. LaCasse, E. C., Mahoney, D. J., Cheung, H. H., Plenchette, S., Baird, S., and Korneluk, R. G. (2008) IAP-targeted therapies for cancer. *Oncogene* **27,** 6252–6275 CrossRef Medline
59. Fulda, S. (2015) Promises and challenges of Smac mimetics as cancer therapeutics. *Clin. Cancer Res.* **21,** 5030–5036 CrossRef Medline
60. Cheung, H. H., Mahoney, D. J., Lacasse, E. C., and Korneluk, R. G. (2009) Down-regulation of c-FLIP enhances death of cancer cells by smac mimetic compound. *Cancer Res.* **69,** 7729–7738 CrossRef Medline
61. Varfolomeev, E., Izrael-Tomasevic, A., Yu, K., Bustos, D., Goncharov, T., Belmont, L. D., Masselot, A., Bakalarski, C. E., Kirkpatrick, D. S., and Vucic, D. (2015) Ubiquitination profiling identifies sensitivity factors for IAP antagonist treatment. *Biochem. J.* **466,** 45–54 CrossRef Medline
62. Pilling, A. B., Hwang, O., Boudreault, A., Laurent, A., and Hwang, C. (2017) IAP antagonists enhance apoptotic response to enzalutamide in castration-resistant prostate cancer cells via autocrine TNF-α signaling. *Prostate* **77,** 866–877 CrossRef Medline
63. Sumi, H., Inazuka, M., Hashimoto, K., Ishikawa, T., Yoshida, S., and Yabuki, M. (2016) T-3256336, a novel and orally available small molecule IAP antagonist, induced tumor cell death via induction of systemic TNFα production. *Biochem. Biophys. Res. Commun.* **479,** 179–185 CrossRef Medline
64. Petersen, S. L., Wang, L., Yalcin-Chin, A., Li, L., Peyton, M., Minna, J., Harran, P., and Wang, X. (2007) Autocrine TNFα signaling renders human cancer cells susceptible to Smac-mimetic-induced apoptosis. *Cancer Cell* **12,** 445–456 CrossRef Medline
65. Bai, L., McEachern, D., Yang, C. Y., Lu, J., Sun, H., and Wang, S. (2012) LRIG1 modulates cancer cell sensitivity to Smac mimetics by regulating TNFα expression and receptor tyrosine kinase signaling. *Cancer Res.* **72,** 1229–1238 CrossRef Medline
66. Raam, S., Richardson, G. S., Bradley, F., MacLaughlin, D., Sun, L., Frankel, F., and Cohen, J. L. (1983) Translocation of cytoplasmic estrogen receptors to the nucleus: immunohistochemical demonstration utilizing rabbit antibodies to estrogen receptors of mammary carcinomas. *Breast Cancer Res. Treatment* **3,** 179–199 CrossRef Medline
67. Maruvada, P., Baumann, C. T., Hager, G. L., and Yen, P. M. (2003) Dynamic shuttling and intranuclear mobility of nuclear hormone receptors. *J. Biol. Chem.* **278,** 12425–12432 CrossRef Medline